

## Ratio of Wheel/Rail Steel Hardness that Ensures Minimum Wear

Azamat Kanayev<sup>a,\*</sup>, Amangeldy Kanayev<sup>b</sup>, Aliya Moldakhmetova<sup>c</sup>

<sup>a</sup>Department of Scientific Projects and Publications, L. Gumilyov Eurasian National University, 2 Satbayev St., Astana, Kazakhstan,

<sup>b</sup>Department of Standardization, Metrology and Certification, S. Seifullin Kazakh Agrotechnical Research University, 62 Zhenis St., Astana, Kazakhstan,

<sup>c</sup>Department of Scientific Projects and Publications, L. Gumilyov Eurasian National University, 2 Satbayev St., Astana, Kazakhstan.

### Keywords:

Wheel  
Rail  
Hardness ratio  
Plasma quenching  
Crack resistance  
Martensite  
Troostite  
Sorbite

### ABSTRACT

Different variants of the hardness of the wheel/rail friction pair were investigated to determine the optimal hardness range of the wheel/rail that ensures the minimum wear under selected test conditions. A pair of tests was performed on an MI-2 machine with a cylindrical wheel steel roller and a rail steel liner. The hardness of the wheel steel specimens ranged from 275 to 900  $HV_w$ . The selected of the rail steel samples of 345-455  $HV_r$  covers the possible hardness variations (350-405  $HV_r$ ) of R65 type long rails produced on the standard ST RK 2432-2013 "Railway Rails Differentially Hardened and Non-heat-strengthened." Technical Requirements. The optimal ratio of wheel/rail hardness, which ensures minimum wear due to weight loss of the tested samples, is the interval  $HV_w/HV_r-1.41-1.59$ . This ratio of wheel/rail hardness is practically confirmed when linear wear is determined by micrometric measurement of the impression size with  $HV_w/HV_r-1.39-1.56$ . The results of the laboratory tests and the suggestions for the optimal ratio of wheel/rail hardness to improve wear resistance should be verified under field conditions. Oscillography of the destruction process of plasma-hardened and non-strengthened specimens was performed to evaluate the resistance to crack initiation and propagation.

\* Corresponding author:

Azamat Kanayev   
E-mail: [azamat.kanayev@yandex.kz](mailto:azamat.kanayev@yandex.kz)

Received: 5 March 2023

Revised: 3 May 2023

Accepted: 4 June 2023

© 2023 Published by Faculty of Engineering

### 1. INTRODUCTION

One of the factors that determine the development of the country's economy is railway transportation. In fact, approximately 70% of all shipments in the Republic of Kazakhstan, the ninth largest country in the world by area, are delivered to consignees by rail. Under these

conditions, improving the performance and durability of long-distance mainline rolling stock wheel pairs is a major and pressing challenge.

An analysis of the durability of the wheel-rail friction pair shows frictional forces cause wear of these associated products. These forces cause

repeated deformation of contact surfaces, their hardening and softening, heat generation, changes in microstructures and substructure, adhesion development, fatigue, corrosion, and other physical and chemical processes. The complexity of these processes in the contact zone has led to various theories of external friction and wear. To date, no unified theory has been developed to explain the wear mechanism in a wheel-rail friction pair [1-3].

The lack of a single theory explaining the wear mechanism and various factors simultaneously affecting complex wear processes of wheels and rails led to the hypothesis that the main reason for severe wear and significant shortening of the service life of wheel pairs is a violation of the optimal wheel-rail hardness ratio. It is emphasized that an excessive difference in hardness between these relevant elements should not be allowed to avoid an undesirable transfer of the greatest wear to one of the elements of the friction pair [4,5].

Practice shows that there is no firmly defined optimal wheel/rail hardness ratio (mandatory equality of hardness, mandatory over-hardening of one element regarding the other by a fixed percentage, etc.) [6,7].

According to [8], specially prepared laboratory tests of wheel specimens with a slip ratio of 2% gave a minimum value of 1.2 (20% higher than rail hardness). However, the results used to determine the required hardness ratio of the wheel-rail pair, and the hypothesis concerning the causes of severe wear of the wheel pairs (violation of the required hardness ratio), do not agree well with practice in actual performance conditions. As a result, the hardness ratio of the friction between the wheels and the rails is currently the subject of lively debate among scientists and engineers. There is an ongoing debate about the optimal hardness ratio of the wheel and rail [9,10]. Obtaining direct experimental data for optimizing rail and wheel hardness in field tests is a complex technological and economic goal. This is because industrial tests are characterized by a long duration and a high labor cost because of the need to develop the performance resources of the wheel-rail friction pair, its periodic disassembly when worn, and the complexity of measuring wear of wheels and rails.

## 2. MATERIALS AND RESEARCH METHODS

In this study, the relationship between the hardness of the wheel and the rail and the wear resistance was investigated in laboratory conditions [11,12] with the MI2 machine, which allows to determine the wear when the wheel slides only on the rail (wear of the first type). Figure 1 shows the schematic of the cylindrical roller and liner wear test to determine the volumetric wear. We used roller samples with a diameter of 40 mm and a width of 10 mm cut from a plasma hardened wheel with a plasma quencher, UDGZ-200.

The elemental composition of wheel steel in wt.% (0.64 C; 0.70 Mn; 0.28 Si; 0.017 P; 0.020 S) and rail steel (0.81 C; 0.95 Mn; 0.26 Si; 0.017 P; 0.015 S) meets the standard - GOST10791-2011, ST RK 2432-2013 [13,14]. The hardness of the wheels after plasma hardening of the samples varied between 275 HV and 850 HV. Note that the advantage of this heat treatment is the residual compressive stresses on the surface layer of the wheel, which increases the contact fatigue strength (crack resistance) of the wheel [15,16].

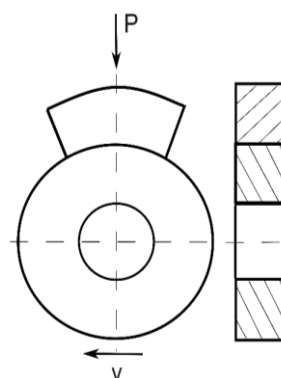


**Fig. 1.** Diagram of the wear test of cylindrical roller and liner.

We used liners with a thickness of 5 mm and a width of 10 mm made of rail steel as a counter body according to ST RK 2432-2013 "Railway Rails Differentially Hardened and Non-heat-strengthened." Wear test mode: pressure (load) between specimens 688 N (70 kg) and roller shaft speed of 500 rpm. Both specimens remained free of defects during the baseline test. The selected hardness of the specimens (both wheels and rails) can be determined under real rolling stock field conditions, resulting in laboratory tests that are closer to real life and have considerable practical importance.

Wear resistance was determined by weighing the mass of the sample before and after the test. Wear was measured as the mass loss of the sample, for which the sample was weighed before and after the test to an accuracy of 0.0002 g. Mass loss  $g \times m^2/t$ , where  $g$  is the mass loss (g),  $m^2$  is the wear area, and  $t$  is wear time. Measuring the wear rate by weight loss is a complex problem, which is a disadvantage of this method. This drawback was eliminated by micrometric measurements using an instrument microscope before and after wear. Hence, the method for determining wear by weight loss (volumetric wear) was duplicated by micrometric measurement of the size of the indentation applied to the surface of the specimen (linear wear).

## 2.1 Determination of the linear wear by reduction of the indentation

As mentioned earlier, measuring wear due to weight loss is a complex problem that takes a lot of time. Thus, a micrometric measurement method was used, which has been successfully applied to determine linear wear. This method is based on accurate micrometric measurements of impression size using instrument microscopes before and after wear of test specimens. The essence of the method is that indentations are made on the working surface, by reducing which the extent of linear wear is assessed (Figure 2).

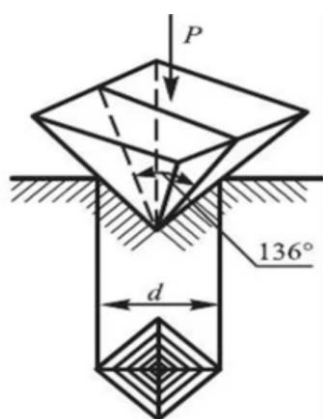


Fig. 2. Diagram of the diamond pyramid impression.

We indented the working surface with a quadruple diamond pyramid with a square base and a  $136^\circ$  apex angle between opposing faces. The pyramids were made with the PMT-3 microhardness tester and reduction in indentation was measured.

The impression depth  $h$  was determined using the formula:

$$h = \frac{d}{2} \sqrt{2 \tan \frac{\alpha}{2}} \quad (1)$$

where  $\alpha$  is the angle at the pyramid apex between opposite faces and  $d$  is the length of the impression diagonal. When  $\alpha = 136^\circ$ ,  $h = 0.143d$ . Linear wear is defined as the difference in the indentation's depth before and after the test  $\Delta h = h_1 - h_2 = 0,143(d_1 - d_2)$  at  $\alpha = 136^\circ$ , where  $h_1$  is the impression depth before the test,  $h_2$  is the same after the test.

The attractiveness of this method when using impressions applied with the microhardness tester PMT-3 make it possible to evaluate the wear intensity of individual structural and phase components of steel (e.g., pearlite, ferrite, cementite, and carbides) if the particle sizes allow microhardness impressions to make on them (Figure 3). The accuracy of linear wear measurement by microhardness impressions before and after wear was 0.3 mm. The diagonals of the impression ranged from 1 to 10  $\mu\text{m}$ .

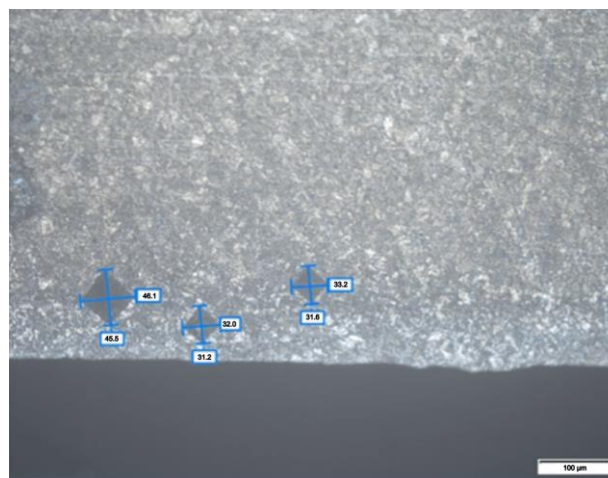


Fig. 3. Measuring the length of the diagonals of impressions with the Thixomet (x 20).

In this method, linear wear is determined with the Thixomet software, a digital image analyzer that allows a user to obtain the required information automatically, which increases the objectivity and accuracy of the estimation.

## 3. RESULTS AND DISCUSSION

Table 1 shows the results of tests to determine the optimal hardness range in the wheel-rail friction pair for rails with a surface hardening of

345-455 HV. Note that this hardness range covers possible hardness variations (350-405 HV) of R65 type long rails, DT 350 category, produced by Aktobe Rail and Section Works according to ST RK 2432-2013 "Railway Rails Differentially Hardened and Non-heat-strengthened." Technical Requirements.

The hardness of the wheel samples varied from 275 to 900 HV<sub>w</sub> (Table 1). The depth of the plasma hardened layer for the wheel steel specimens was ~1.5 mm. The hardness values of the wheel-rail specimens can be obtained by varying the plasma quench current, the length of the plasma arc, and the diameter of the ceramic nozzle.

From the data in Table 1, the minimum total wear decreases with the ratio of hardness of wheel and rail HV<sub>w</sub>/HV<sub>r</sub> from 1.41 to 1.59. The wear of wheel specimens in the hardness range 275-505 HV<sub>w</sub> (HV<sub>w</sub>/HV<sub>r</sub> ratio=0.80-1.35) is 2.2 times greater than in the hardness range 560-675 HV<sub>w</sub> (HV<sub>w</sub> / HV<sub>r</sub> ratio=1.41-1.59). To obtain a complete picture of wear resistance of the wheel and rail, we used samples whose hardness exceeds the limits set by the standard in the experiments. Similarly, the data in Table 1 show that wear of the wheel steel specimens increases when they are hardened to a high hardness (860-900 HV), which can lead to pitting and cracking in the hardened layer.

**Table 1.** Effect of the wheel-rail hardness ratio on wear resistance of wheel-metal and rail-metal pair.

| N | Wheel hardness, HV <sub>w</sub> | Rail hardness, HV <sub>r</sub> | Hardness ratio, HV <sub>w</sub> / HV <sub>r</sub> | Volumetric wear specimen, g |            |            |
|---|---------------------------------|--------------------------------|---|-----------------------------|------------|------------|
|   |                                 |                                |   | wheel steel                 | rail steel | total wear |
| 1 | 263                             | 430                            | 0.61  | 1.10                        | 0.21       | 1.31       |
| 2 | 275                             | 345                            | 0.80  | 0.95                        | 0.24       | 1.19       |
| 3 | 380                             | 362                            | 1.05  | 0.73                        | 0.26       | 0.99       |
| 4 | 505                             | 377                            | 1.35  | 0.58                        | 0.22       | 0.80       |
| 5 | 560                             | 397                            | 1.41  | 0.37                        | 0.23       | 0.60       |
| 6 | 615                             | 410                            | 1.50  | 0.33                        | 0.25       | 0.58       |
| 7 | 675                             | 425                            | 1.59  | 0.29                        | 0.21       | 0.50       |
| 8 | 860                             | 440                            | 1.95  | 0.48                        | 0.44       | 0.92       |
| 9 | 900                             | 455                            | 1.98  | 0.51                        | 0.49       | 1.00       |

Hardening of wheel rims and flanges to a relatively low hardness of 259-551 HV is ineffective because wear resistance is only slightly improved. Note that a clearer picture requires a further in-depth analysis of the

hardness range, considering external (slippage, friction coefficient, lubrication, etc.) and internal (elemental composition, especially carbon, microstructure, strength, etc.) factors [6,17-19].

Micrometric measurements to determine linear wear show that the optimal range for wheel hardness is between 555-655 HV, i.e., the optimal ratio of wheel-rail hardness HV<sub>w</sub>/HV<sub>r</sub> is between 1.39-1.56. The linear wear of both wheel and rail specimens has a minimum of 3.1-3.8 μm, and the total wear decreases by ~1.5-2.0 times. Increasing the wheel hardness by over 868 HV results in intense wear of both the wheel (5.1 μm) and the rail (4.6 μm). Strengthening the rim to hardness 370-450 HV is ineffective because wheel wear in this hardness range is: ~2.0 times greater than in the hardness range of 555-565 HV. We can note that the wear of the samples of wheel and rail steel increases with the ratio HV<sub>w</sub> / HV<sub>r</sub> = 1.95 (Table 2).

With the surface hardness of the wheel 555-655 HV<sub>w</sub> and the surface hardness of the rail 400-420 HV<sub>r</sub>, the optimal hardness ratio of the wheel and rail HV<sub>w</sub>/HV<sub>r</sub>, which ensures minimum linear wear (under test conditions), is between 1.39-1.56. It is practically the same as the ratio of the hardness of the wheel and rail in the determination of volumetric wear HV<sub>w</sub>/HV<sub>r</sub>–1.41-1.59.

**Table 2.** Determination of linear wear by micrometric measurements with instrument microscopes before and after specimen wear.

| N | Wheel hardness, HV <sub>w</sub> | Rail hardness, HV <sub>r</sub> | Hardness ratio, HV <sub>w</sub> / HV <sub>r</sub> | Linear wear specimen, g |            |            |
|---|---------------------------------|--------------------------------|---|-------------------------|------------|------------|
|   |                                 |                                |   | wheel steel             | rail steel | total wear |
| 1 | 271                             | 427                            | 0.63  | 10.0                    | 3.2        | 13.2       |
| 2 | 370                             | 395                            | 0.94  | 9.6                     | 3.5        | 13.1       |
| 3 | 394                             | 375                            | 1.05  | 7.7                     | 3.3        | 11.0       |
| 4 | 450                             | 380                            | 1.18  | 6.8                     | 3.2        | 10.0       |
| 5 | 555                             | 400                            | 1.39  | 3.5                     | 3.1        | 6.6        |
| 6 | 604                             | 411                            | 1.47  | 3.1                     | 3.3        | 6.4        |
| 7 | 655                             | 420                            | 1.56  | 3.8                     | 3.5        | 7.3        |
| 8 | 868                             | 445                            | 1.95  | 5.1                     | 4.6        | 9.7        |

Since the tests performed do not provide a clear solution to the problem of increased wear intensity, further studies are needed to select the optimal ratio at which the optimal ratio of mechanical properties of wheel and rail steel can be achieved.

A critical analysis of the results of a series of tests carried out shows that, depending on the initial condition of the samples and many external (coefficient of friction, lubrication, slippage, etc.) and internal (carbon content, hardness, microstructure, etc.) factors, there is a certain hardness range of the wheel-rail friction pair, in which wear has a minimum value.

While increasing the wear resistance of the wheels, it is also necessary to ensure high resistance to the nucleation and propagation of cracks. We tested impact bending using an oscillograph that records the cracking process in the force-time coordinates (Figure 4). Analysis of oscillograms and the fractographic studies of the specimen fractures show the fundamental difference between the fracture pattern nature of hardened specimens and non-strengthened wheel metal.

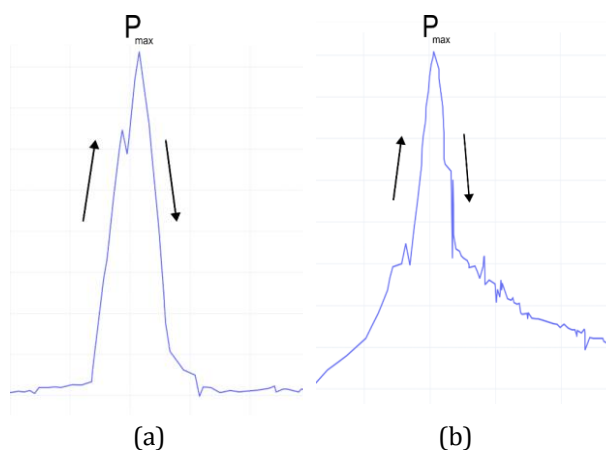
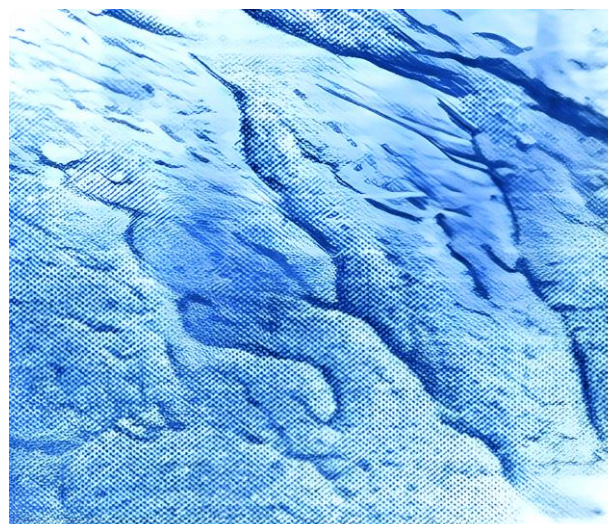


**Fig. 4.** Fracture oscillograms of wheel specimens with plasma quenching (a) and without quenching (b).

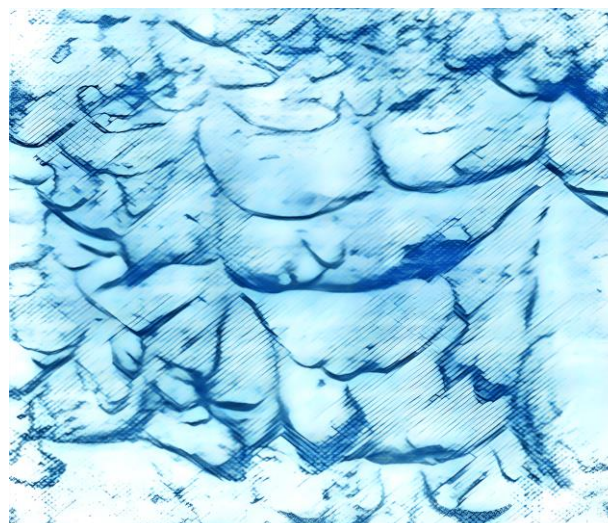
The oscillograms show that the wheel metal, which has no hardened layer, fractures across the cross section, and the fracture process proceeds in two stages, crack initiation and crack propagation, until the specimen fails completely. Figure 4a shows the upward curve (fracture force up to 9.5 kN) and the downward curve to zero at crack propagation. This fracture mechanism is due to the homogeneous structure of the metal in the fracture cross section. This ensures that the mechanical properties of the metal are the same over the cross section. During plasma quenching, when the metal comprises two layers – a hardened (brittle) layer and an original (ductile) layer – the fracture process follows a “multiple” mechanism. The crack starts at the surface of the hardened layer (as seen in the oscillogram at lower forces) and grows in depth, until it stops at

the boundary with the original soft metal, since it requires a much higher force to propagate further than the initiation in the hardened layer.

As the grain size decreases, the stress concentration at the boundary decreases, which leads to an increase in the fatigue limit. From this point of view, plasma treatment of wheel metal provides the most energy-intensive mechanism, which should have a positive effect on the performance characteristics of the metal [20,21].



(a)



(b)

**Fig. 5.** Electronic microfractograms (x 5000) of brittle and ductile wheel steel fractures. (a) Brittle (streamlike) fracture; (b) Ductile fracture (cupular).

Fractograms confirm the fracture patterns resulting from the sample. For example, non-strengthened wheel metal is characterized by a brittle intragranular chip (Figure 5a) with a distinct streamlike pattern. This is a system of

converging fracture stages. A quasi-chip characterizes the wheel metal with a strengthened layer. The size of the chipping facets (smooth surfaces) is much smaller than the chipping facets of the non-strengthened metal, that shows high dispersion in structure of the strengthened layer (Figure 5b).

One of the main reasons for increased crack resistance is an improvement in martensite dispersion, i.e., martensite crystal refinement.

Analysis of the fracture microstructure at high magnification shows that volume-hardened martensite fractures predominantly by splitting at the original austenitic grain boundaries. This is favored by the segregation of embrittlement inclusions (carbides, sulfides, nitrides) at these boundaries since grain boundaries with segregated impurities provide a more energetically favorable crack path.

The refinement of martensitic grains in plasma quenching results from a reduction of the original austenitic grain size because of ultrafast heating rates (1500-3000°C/s) and cooling rates (700-800°C/s), and the metal remains at high temperatures ( $10^{-2}$ - $10^{-4}$  s) for a short time. This is fully consistent with known findings about the positive effect of increasing the heating rate and shortening the austenitization time on improving the material strength and resistance to brittle fracture [22,23].

Notably, the physical theory of metal fracture can also explain the improvement in crack resistance and the positive effect of increasing dispersion on crack strength [24]. According to this theory, the critical stress  $\sigma_{cr}$  is inversely proportional to the grain size  $d$ .

$$\sigma_{cr} = kd^{1/2} \quad (2)$$

The qualitative transition from a coarsely acicular martensitic microstructure in conventional volumetric hardening to a highly dispersed finely acicular microstructure in plasma processing also drives a qualitative change in fracture micromechanism, i.e., a transition from intergranular fracture to intragrain fracture.

Besides obtaining a more favorable martensitic structure, another reason for improved crack resistance with plasma quenching is the gradient

troostite/sorbite heterostructure between the hardened surface and the volume hardened soft tempered zone. The size of the temperature interval between the austenitic and martensitic ( $\gamma \rightarrow \alpha$ ) transformation determines the length between the quenched and tempered zone [25-27].

Fracture of specimens after double (plasma and volumetric) quenching happens through a multiple mechanism with crack inhibition at the boundary with the tempering zone by a curved trajectory. The reasons for crack inhibition are the transition of residual stress in this zone from compressive to tensile and the high plasticity of the material of the tempering zone compared to the hardened zone. This mechanism of crack inhibition and the curvature of the trajectory are consistent with data obtained for other surface hardening processes characterized by a sharp boundary between zones with different metal structures during nitriding, nitrocarburizing, and other processing.

These test results show that surface plasma hardening can be used effectively for volume-hardened components [28,29]. This process, which is not possible with conventional volumetric hardening methods, can improve the hardness of the working surface and crack resistance at the same time.

#### 4. CONCLUSIONS

1. The optimal ratio of wheel and rail hardness, which ensures minimum wear due to the loss of weight of the tested specimens, is in the interval  $HV_w/HV_r$ -1.41-1.59. This ratio of wheel and rail hardness is practically confirmed when linear wear is determined by measuring the size of the indentation  $HV_w/HV_r$ -1.39-1.56. From the point of view of cost reduction in wheel repair, a more accurate and objective ratio of 1.39 is the most acceptable since this value of wheel steel hardness (555 HV) does not cause difficulties in machining.
2. Wear of wheel steel specimens worsens when hardened to a high hardness (above 860 HV), which can lead to pitting and cracking in the hardened layer. Hardening the wheel to a relatively low hardness (275-505 HV) is ineffective, as wear resistance improves slightly.

3. The results of the laboratory test and the suggestions for the optimal hardness ratio of the wheel/rail pair for wear resistance should be verified under field conditions.
4. Fracture oscillography of the specimens, performed to evaluate their resistance to crack initiation and propagation, shows that the metal of the wheel, which has no strengthened layer because of the uniformity of the structure, fractures over the entire cross section. The fracture process proceeds in two stages — crack initiation and propagation until the complete failure of the specimen.
5. Plasma quenching can be used effectively for components and products operated in the volume-hardened condition. A simultaneous increase in surface hardness and crack resistance is achieved, which is practically impossible with conventional methods of independent volume and surface hardening.

## REFERENCES

- [1] V.M. Bogdanov, S.M. Zakharov, *Modern Problems of Wheel-Rail System*, World Railroads, vol.1, pp. 57-62, 2014.
- [2] Z. Wanming, J. Xuesong, W. Zenfeng, Z. Xin, *Wear problems of high-speed wheel/rail systems: Observations, Causes, and Countermeasures in China*. Applied Mechanical Review, vol.72, iss. 6, 2020, pp. 1-23, doi: [10.1115/1.4048897](https://doi.org/10.1115/1.4048897)
- [3] IX World Congress on High-speed Rail Traffic, 7-10 July, 2015, Tokyo, Japan.
- [4] S. Seetharaman, *Fundamentals of Metallurgy*, Elsevier Science, 2005.
- [5] L.I. Kuksenkova, S.A. Polykov, *The Problems of Materials Science and Their Methodological Features in the Science of Friction and Wear*, Metal Science and Heat Treatment, no. 3, pp. 3-12, 2021, doi: [10.30906/mitom.2021.3.3-12](https://doi.org/10.30906/mitom.2021.3.3-12) (in Russian)
- [6] E.A. Shur, *To a question on optimal ratio of rails and wheels hardness*, in Scientific and Technical Conference, in Modern Problems of interaction of rolling stock and track, pp. 87-93, 2003, (in Russian)
- [7] W. Hu, M. Watson, M. Maiorino, L. Zhou, W.J. Wang, H.H. Ding, R. Lewis, E. Meli, A. Rindi, Q.Y. Liu, J. Guo, *Experimental Study on Wear Properties of Wheel and Rail Materials With Different Hardness Values*. Wear, vol. 477, 203831, 2021, doi: [10.1016/j.wear.2021.203831](https://doi.org/10.1016/j.wear.2021.203831)
- [8] T.V. Larin, *On Optimal Hardness of Elements of Friction Pair "Wheel-rail"*, Proceedings of Higher Education, Ferrous Metallurgy, no. 10, pp. 4-9, 1986. (in Russian)
- [9] X. Shi, Q. Yan, X. Zhang, G. Diao, C. Zhang, Z. Hong, Z. Wen, X. Jin, *Hardness Matching of Rail/wheel Steels for High-speed-train Based on Wear Rate and Rolling Contact Fatigue Performance*, Materials Research Express, vol. 6, 2019, doi: [10.1088/2053-1591/ab072d](https://doi.org/10.1088/2053-1591/ab072d)
- [10] A.M. Vikhrova, T.V. Larin, Yu.M. *On Hardness Ratio of Rail and Wheel Steel*, Proceedings of Higher Education, Ferrous Metallurgy, no. 5, pp. 34-38, 1987. (in Russian)
- [11] M.L. Bernshtein, G.M. Rakhshadt, *Metallurgy and Heat Treatment of Steel, Handbook*, 3rd edition, vol. 1 Tests and Research Methods, Moscow, Metallurgy, 1983.
- [12] A. Cottrell, *Introduction to Metallurgy*, 2<sup>nd</sup> Edition. London, CRC Press, 2019.
- [13] Interstate standard GOST 10791-2011, *Solid-rolled Wheels, Technical Conditions*, 2011.
- [14] Ministry of Investment and Development of the Republic Kazakhstan, ST RK 2432-2013 Differentially Hardened and Non-Heat-Strengthened Railway Rails, available at: <https://pdf.standartgost.ru/catalog/Data2/1/4293741/4293741095.pdf> (in Russian)
- [15] A.V. Sukhov, S.L. Shitkin, *Prospects for X-ray Method of Residual Stress Control in Solid Rolled Wheels*, in G.V. Gogrichiani (Ed.): Perspective Problems of Railway Transport Development, Intext, Moscow, pp. 244-253, 2010
- [16] European standard EN 13262-2004, *Railway Applications, Wheels and Bogies, Wheels, Product Requirements*, 2004
- [17] U. Spangenberg, R.D. Fröhling, P.S. Els, *The Effect of Rolling Contact Fatigue Mitigation Measures on Wheel Wear and Rail Fatigue*, Wear, vol. 398-399, pp. 56-68, 2018, doi: [10.1016/j.wear.2017.11.012](https://doi.org/10.1016/j.wear.2017.11.012)
- [18] R. Lewis, P. Christoforou, W.J. Wang, A. Beagles, M. Burstow, S.R. Lewis, *Investigation of the Influence of Rail Hardness on the Wear of Rail and Wheel Materials Under Dry Conditions (ICRI Wear Mapping Project)*, Wear, vol. 430-431, pp. 383-392, 2019, doi: [10.1016/j.wear.2019.05.030](https://doi.org/10.1016/j.wear.2019.05.030)
- [19] L.A. Sladkova, A.N. Neklyudov, *New Look at the Problem of Rolling Stock Wheel Wear*, Journal of Friction and Wear, vol. 42, no. 2, pp. 162-169, 2021, doi: [10.32864/0202-4977-2021-42-2-162-169](https://doi.org/10.32864/0202-4977-2021-42-2-162-169)

- [20] P.G. Adischev, A.S. Tselischev, M.V. Malkov, M.V. Mishukov, A.N. Shishlonova, *Research Direction in Developing New Wear Resistant Steels*, Steel, no. 6, pp. 54-57, 2021. (in Russian)
- [21] S.A. Nikulin, S.L. Shitkin, A.V. Rozhnov, S.O. Rogachev, T.A. Nechaikina, *Application of X-ray Method to Determine Stressed State of Parts of Railway Transport*. Proceedings of Higher Education. Ferrous Metallurgy, Vol. 60, no. 3, pp. 200-206, 2017, doi: [10.17073/0368-0797-2017-3-200-206](https://doi.org/10.17073/0368-0797-2017-3-200-206) (in Russian)
- [22] A.T. Kanaev, A.V. Bogomolov, T.E. Sarsembaeva, *Overall Hardening of Solid-rolled Wagon Wheels by Volume Quenching and Surface Plasma Processing*, Solid State Phenomena, vol. 265, pp. 706-711, 2017, doi: [10.4028/www.scientific.net/SSP.265.706](https://doi.org/10.4028/www.scientific.net/SSP.265.706)
- [23] V.V. Tsyganov, R.E. Mokhnach, S.P. Sheiko, *Increasing Wear Resistance of Steel by Optimizing Structural State of Surface Layer*, Steel in Translation, vol. 51, pp. 54-57, 2021, doi: [10.3103/S096709122102011X](https://doi.org/10.3103/S096709122102011X)
- [24] A.H. Cottrell, *Theoretical Aspects of the Fracture Process*, in *Atomic Mechanism of Fracture*. Translated from English, Moscow, Metallurgizdat, pp. 30-58, 1963. (in Russian)
- [25] V.E. Kosterev, O.Y. Efimov, Y.F. Ivanov, *Formation of Gradient Structural-phase States During Thermomechanical Hardening*. Proceeding of Higher Education. Ferrous Metallurgy, no. 4, pp. 24-27, 2018, doi: [10.17073/0368-0797-2017-6-457-462](https://doi.org/10.17073/0368-0797-2017-6-457-462) (in Russian)
- [26] A.V. Brover, *Structural features of the process of surface hardening of steel by highly concentrated energy flows*, Materials Science, no. 9, pp. 18-23, 2005. (in Russian)
- [27] O.V. Chudina, V.M. Prikhodko, Yu.M. Luzhnov, *Structural Aspects of Surface Hardening of Parts Working in Wear Conditions*, Strengthening Technologies and Coatings, vol. 18, no. 9, pp. 396-404, 2022, doi: [10.36652/1813-1336-2022-18-9-396-404](https://doi.org/10.36652/1813-1336-2022-18-9-396-404) (in Russian)
- [28] V.G. Efremenko, K. Shimizu, T.V. Pastukhova, Y.G. Chabak, A.V. Efremenko, K. Kusumoto, *Wear Mechanism and Chemical Composition Optimization of Complex-alloyed Cast Iron With Spheroidal Vanadium Carbide Under Conditions of Abrasive Erosion*, Journal of Friction Wear, vol. 38, iss. 1, pp. 58-64, 2017, doi: [10.3103/S106836661702009X](https://doi.org/10.3103/S106836661702009X)
- [29] A.V. Bogomolov, A.T. Kanaev, T.E. Sarsembaeva, *Determination of Mechanical Characteristics Plasma Hardened Wheel Steel*, IOP Conference Series: Materials Science and Engineering, vol. 969, 2020, doi: [10.1088/1757-899X/969/1/012037](https://doi.org/10.1088/1757-899X/969/1/012037)